tive value of ν, in that event the quadratic equation

$$\psi_j = A_j + B_j\nu + C_j\nu^2 \tag{12}$$

is used to estimate a crossover value of ν. The coefficients A_j, B_j and C_j of Eq. (12) are computed for a curve which passes through point B of Fig. 1 and has the same first and second derivatives ($d\psi^0/d\nu$ and $d^2\psi^0/d\nu^2$) at that point. The quadratic curve does not necessarily go through the origin or the point A. The coefficients of Eq. (12) may be expressed in the forms

$$2C_j = d^2\psi_j{}^0/d\nu^2 \tag{13}$$

$$B_j = (d\psi_j{}^0/d\nu - 2C_j\nu_0) \tag{14}$$

and

$$A_j = \psi_j{}^0 - B_j\nu_0 - C_j\nu_0{}^2 \tag{15}$$

The zero roots of Eq. (12) may be found by substituting C_j, B_j, and A_j from Eqs. (13-15) into Eq. (11). If the roots for a given mode are not real and positive, then the curve fit for that mode fails.

Examples

Data for Eq. (1) was generated for the cantilevered box beam of Ref. 3 where the design parameters were those listed in Table I of that reference. The number of generalized coordinates was six. Computations were carried out on an IBM 360 model 50 machine.

A digital computer program was written which implemented the flutter velocity solution method described in Sec. 2. For the previously mentioned box beam an initial value of $\nu_0 = 1$ was assumed and the program found a flutter velocity of 869.8 fps at $\nu = 10.15$, for a tolerance ϵ equal to 0.05. The computations of the flutter velocity were repeated for values of $\nu_0 = 2, 3, \ldots, 20$. In each case the program converged to a flutter velocity between 868.2 and 870.5 for values of ν between 10.12 and 10.16. The time for the 20 flutter velocity calculations was 210.83 sec, or an average of 10.54 sec/flutter velocity analysis. For initial values of ν_0 equal to 8 and 9 the algorithm converged to an answer on the first attempt; the required time was 3.91 sec for each flutter velocity analysis. The critical mode was 2.

The flutter velocity analyses were repeated for design parameters of the box beam equal to 1/6 of the values cited in Table I of Ref. 3. The results of the flutter velocity analyses were similar to those described in the preceding paragraph.

The method was employed in the optimum design of the same box beam with six degrees of freedom and twelve design parameters of Ref. 3. ϵ was 0.05 and the total computer run time for arriving at approximately the same relative optimum design parameters of the second example of Ref. 5 was 8 min 0.00 sec. The program did not experience any convergence problems. The previous run time reported in Ref. 5 was 9 minutes 42.68 sec.

Discussion

For the first examples presented here the flutter velocity analysis program always converged to an answer for initial values of ν_0 chosen between 1 and 20 and did not show any tendency to diverge from the solution, although the curves for χ_2 and χ_3 crossed at ν equal to 8.71 where the subscripts of ψ_2 and ψ_3 switched. In the second example subscript switching did not occur for the critical mode; however, in the optimization program subscript switching occurred during several of the redesign cycles, without any noticeable effect on the efficiency or accuracy of the program.

The method for finding the flutter velocity which was presented here should be applicable to any aeroelastic flutter theory. The procedure is simple in concept and was trouble free for the examples cited.

Appendix

Equations for the first and second partial derivatives of the eigenvalues with respect to the design parameters were derived by Rudisill and Bhatia.[5] The first and second total derivatives of the eigenvalues with respect to the reduced frequency may be found by substituting derivatives with respect to the reduced frequency for derivatives with respect to the design parameters in Eqs. (15-19) of Ref. 5, then

$$\frac{d\lambda_j}{dk} = -\lambda_j V_j{}^T \frac{dA}{dk} U_j \tag{1A}$$

where $V_j{}^T[K - \lambda_j(M + A)] = 0$ and

$$\frac{d^2\lambda_j}{dk^2} = -V_j{}^T\left[\frac{2d\lambda_j}{dk}\frac{dA}{dk} + \lambda_j\frac{d^2A}{dk^2}\right]U_j + 2V_j{}^T\left[\lambda_j\frac{dA}{dk}\right]\sum_{\substack{h=1\\h\neq j}}^{n}(V_h{}^T\lambda_j\frac{dA}{dk}U_j)U_h/(\lambda_j - \lambda_h) \tag{2A}$$

where the lengths of U_j and V_j are such that $U_j{}^TU_j = 1$ and $V_j{}^T(M + A)\,U_j = 1$.

Derivatives of $\bar{\lambda}_j$ may be found from the relations

$$\frac{d\bar{\lambda}_j}{dk} = -\frac{1}{\lambda_j{}^2}\frac{d\lambda_j}{dk} \tag{3A}$$

and

$$\frac{d^2\bar{\lambda}_j}{dk^2} = \frac{2}{\lambda_j{}^3}\left(\frac{d\lambda_j}{dk}\right)^2 - \frac{1}{\lambda_j{}^2}\frac{d^2\lambda_j}{dk^2} \tag{4A}$$

References

[1]Lawrence, A. J. and Jackson, P., "Comparison of Different Methods of Assessing the Free Oscillatory Characteristics of Aeroelastic Systems," Current Paper 1084, Dec. 1968, Aeronautical Research Council, England.

[2]Hassig, H. J., "An Approximate True Damping Solution of the Flutter Equation by Determinant Iteration," *Journal of Aircraft*, Vol. 8, No. 11, Nov. 1971, pp. 885–889.

[3]Bhatia, K. G., "An Automated Method for Determining the Flutter Velocity and the Match Point," AIAA Paper 73-195, Washington, D.C., 1973.

[4]Desmarals, R. N. and Bennet, R. M., "An Automated Procedure for Computing Flutter Eigenvalues," AIAA Paper 73-393, Williamsburg, Va., 1973.

[5]Rudisill, C. S. and Bhatia, K. G., "Second Derivatives of the Flutter Velocity and the Optimization of Aircraft Structures," *AIAA Journal*, Vol. 10, No. 12, Dec. 1972, pp. 1569–1572.

Pumping Capacity of Venturi Exhausts

Jacques A. F. Hill* and Philip O. Jarvinen†
Sanders Associates Inc., Nashua, N. H.

Introduction

THE performance of a ram air operated airborne combustion unit or aircraft heater is determined largely by the amount of air which may be forced through the combustor-duct system by the differential air pressure. Venturi exhausts may be used to provide additional pressure drop across the system but may be required to pump gases with densities that differ from the pumping gas. This Note discusses experimental data on the variation of venturi

Received January 30, 1973; revision received April 18, 1973.
Index categories: Nozzle and Channel Flow; Subsonic and Transonic Flow.

* Head, AeroScience Department; now at Naval Ordnance Laboratory, White Oak, Silver Spring, Md. Member AIAA.
† Head, AeroSciences Department. Member AIAA.

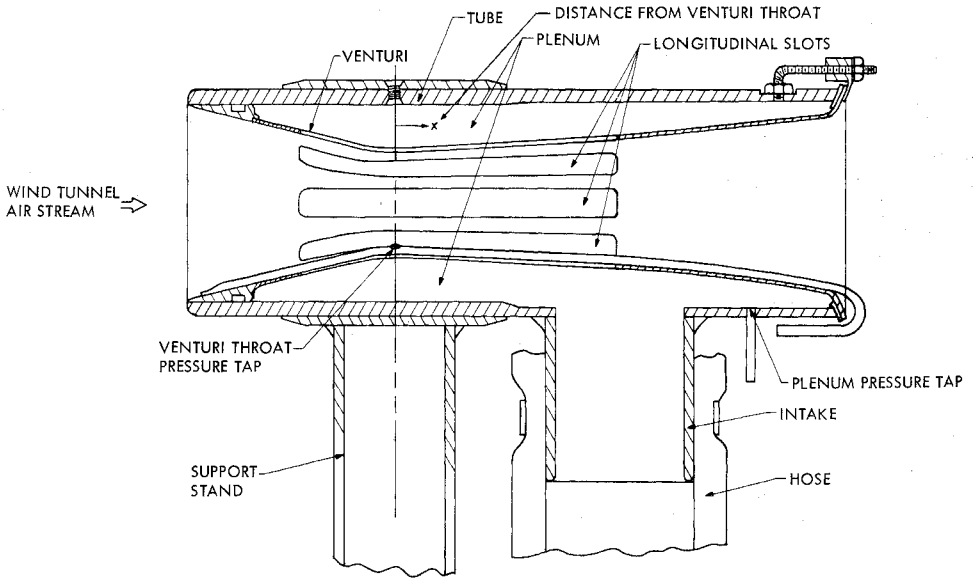

Fig. 1 Test venturi.

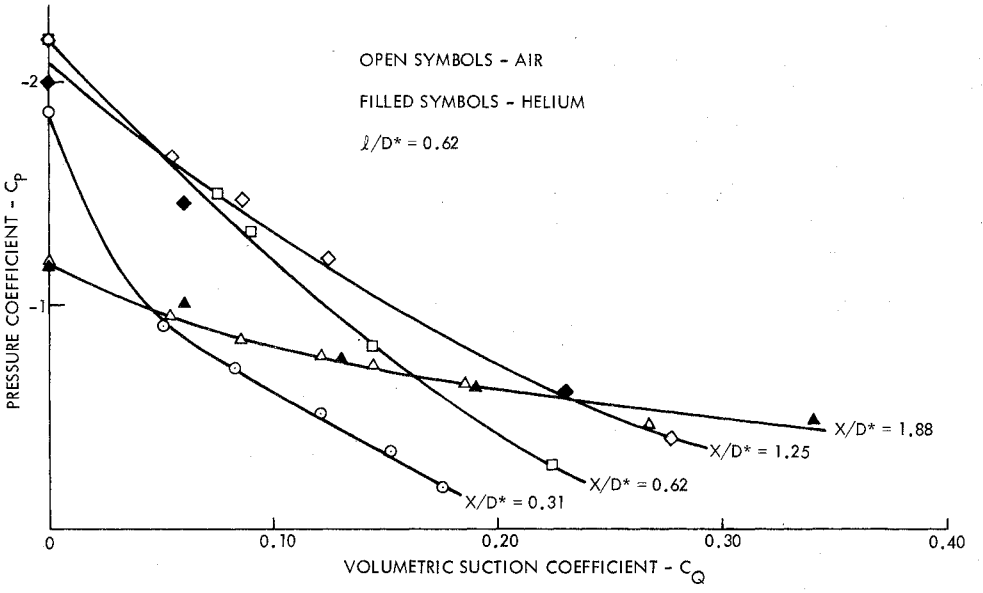

Fig. 2 Venturi pump characteristics.

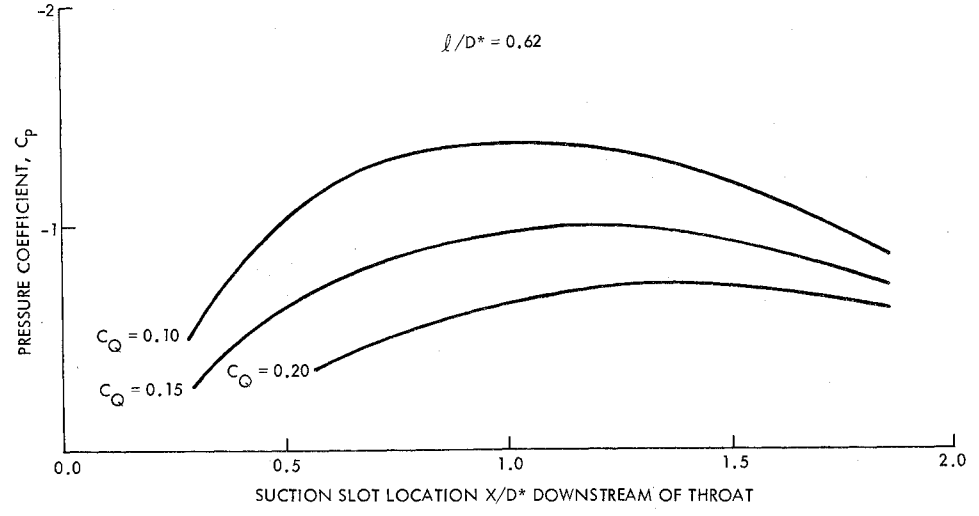

Fig. 3 Suction pressure vs slot location.

suction pressure with pumped gas flow rate, on the optimum location of the pumping orifice in the venturi and on the effect of varying the density of the pumped fluid by using both air and helium gases.

Test Description

The test venturi Fig. 1, ordinarily used for driving gyroscopic flight instruments, has an exit to throat area

ratio of $A_{ex}/A^* = 2.8$ and a throat diameter of 1.63 in. Longitudinal slots were cut as shown to open up about half the perimeter at the throat. These slots extended a constant width both upstream and downstream of the venturi throat. The actual circumferential suction orifice was formed by blocking off all but a short length of the longitudinal slots with tape. The venturi was housed in a tube which formed a plenum for the suction orifice. The pumping connection was through a hose which fitted over a pipe as shown. Outside the wind-tunnel, this hose was connected to another section of pipe containing a valve and flow-metering orifice. The orifice was constructed according to Ref. 1 and has an orifice diameter of 1.48 in., an orifice diameter d to pipe diameter D ratio of 0.60 and 1 D and 1/2 D pressure connections. The orifice flow coefficient K for air and helium flows was in the range 0.66–0.67 and 0.67–0.69, respectively. Pressures were measured at the venturi throat, in the plenum and across the orifice. Provision was made to connect the intake pipe through a pressure-reducing orifice to a pair of helium tanks, manifolded together. The use of helium as the pumped gas provided a density ratio of about 7 with respect to the wind-tunnel stream. The experiment was performed in the MIT Wright Brothers Wind Tunnel at 100 mph.

Experimental Data

The pumping characteristics of the venturi are shown in Fig. 2 in nondimensional form. The pumped flow is given in terms of a volume flow coefficient.

$$C_Q = Q/u_\infty A^*$$

where

Q = the volumetric flow rate
u_∞ = the speed of the airstream
A^* = the cross-sectional area of the venturi throat

The pressures are given in terms of standard pressure coefficients

$$C_p = (p - p_\infty)/q_\infty$$

where

p = the measured pressure in the plenum
p_∞ = the static pressure in the wind tunnel
q_∞ = the dynamic pressure ($\rho u_\infty^2/2$) in the wind tunnel

The reduced data is shown for four longitudinal locations of the suction orifice with the circumferental slot $l/D^* = 0.62$ diameters long. For two configurations ($X/D^* = 1.25$ and 1.88), the air and helium data are shown together and are seen to be in agreement for a given configuration. The pressure coefficient at the venturi throat without injected flow was measured to be $C_p = -3.3$.

A cross plot of all the data taken with a suction slot 0.62 diameters long is shown in Fig. 3 and illustrates the variation of the pressure coefficient with slot location for three values of the volume flow coefficient, C_Q. The optimum location is seen to vary from one diameter to 1.5 diameters downstream of the throat as C_Q increases from 0.1 to 0.20.

Configurations with narrower slots and with asymmetric injection were tested and showed poorer performance than the basic slot configuration.

Conclusions

These tests show that the pumping characteristics of a venturi are invariant with respect to the density of the pumped fluid if the pumping rate is expressed in volumetric terms, the optimum location of a circumferential orifice is of the order of one diameter downstream of the throat and varies with the design flow rate, and a suction-pressure corresponding to $C_p = -1$ (pressure drop seen by the system essentially doubled) is achieved if the pumped volume is limited to 15% of the reference flow through the venturi throat.

Reference

[1]*ASME Power Test Code, Supplement on Instruments and Apparatus*, New York, 1959, Pt. 5, Chap. 4.

The Dynamics of Blade Pitch Control

Maurice I. Young*
The University of Delaware, Newark, Del.

Nomenclature

C	= chord of blade, ft
C_M	= steady aerodynamic moment coefficient
n	= subscript identifying nth blade
0	= subscript indicating initial state
r	= spanwise position along blade, ft
S	= subsidiary variable of the Laplace transformation, rad/sec
t	= time, sec
x,y,z	= rotating Cartesian coordinates, blade principal inertia axes
D_x	= unsteady aerodynamic damping coefficient in pitch, ft-lb-sec/rad
I_x,I_y,I_z	= blade principal mass moments of inertia, slug-ft^2
K	= gain constant of actuator, lb
K_x	= virtual spring constant of centrifugal force field in pitch, ft-lb-sec^2/rad^2
M_{xA}	= aerodynamic pitching moment, ft-lb
M_{xM}	= mechanical pitching moment, ft-lb
N	= number of blades
R	= blade span, radius of rotor, ft
V	= axial velocity in propeller-rotor state, ft/sec
Y	= actuator reference input, ft
σ	= blade geometric pitch angle, rad
λ	= aerodynamic inflow ratio, ratio of axial inflow velocity to blade rotational tip speed
ρ	= density of air, slug/ft^3
τ	= actuator time constant, sec
ψ	= blade azimuth angle, rad
$\omega_x,\omega_y,\omega_z$	= angular velocity components in blade rotating, principal coordinate system, rad/sec
Ω	= steady angular velocity of rotor, rad/sec
1,2	= subscripts referring to longitudinal and lateral control directions
$\bar{(\ )}$	= average value of ( ), Laplace transform of ( )
$\dot{(\ )}$	= differentiation with respect to time
$(\ )'$	= differentiation with respect to azimuth

Introduction

ADVANCED rotorcraft such as the modern helicopter and convertible aircraft utilizing tiltable propeller-rotors frequently employ stability augmentation and gust alleviation devices which require that the pitch settings of the rotor blades be changed both collectively and cyclically in

Received April 20, 1973. Acknowledgment is made of the support of the U.S. Army Research Office under Research Grant ARO-D 31-124-71-G112.

Index categories: Aircraft Handling, Stability, and Control; Rotary Wing Aerodynamics; VTOL Handling, Stability and Control.

*Professor of Mechanical and Aerospace Engineering. Associate Fellow AIAA.